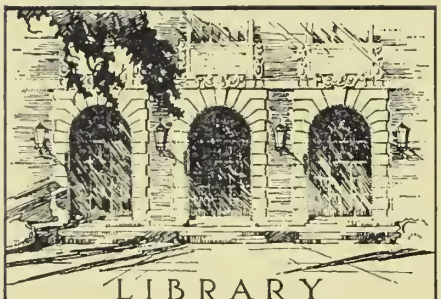

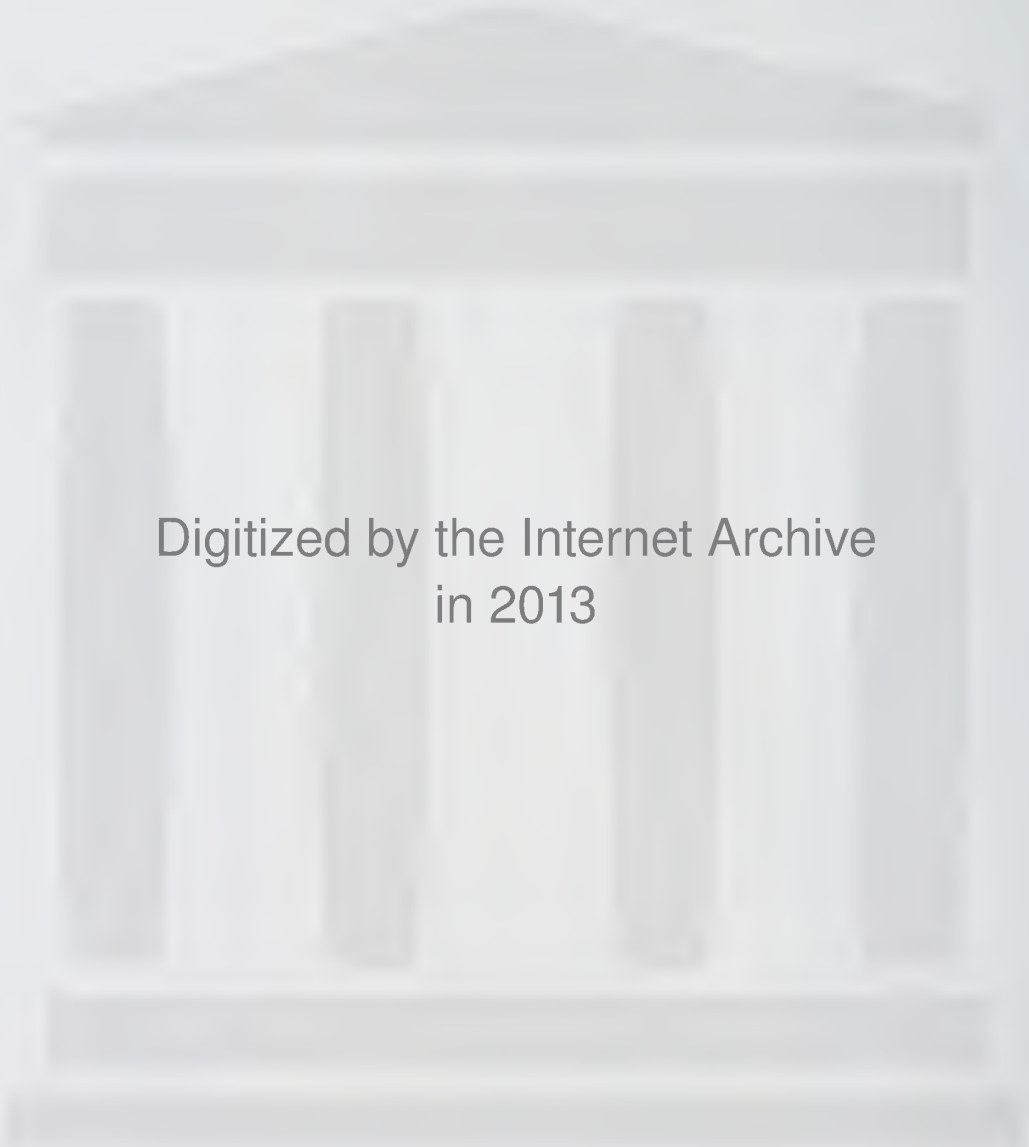

REPORT NO. 358

COO-1018-1192

# MODELING OF DOMAIN GROWTH ACTIVITY IN POLYCRYSTALLINE FERRITES



by

RICHARD PAUL HARMS



November, 1969

DEPARTMENT OF COMPUTER SCIENCE
UNIVERSITY OF ILLINOIS AT URBANA-CHAMPAIGN · URBANA, ILLINOIS

Report No. 358

# MODELING OF DOMAIN GROWTH ACTIVITY IN POLYCRYSTALLINE FERRITES

by

RICHARD PAUL HARMS

November, 1969

Department of Computer Science
University of Illinois
Urbana, Illinois 61801

* Supported in part by Contract Number U.S. AEC, AT(11-1)-1018 and submitted in partial fulfillment for the degree of Master of Science in Electrical Engineering, at the University of Illinois, November, 1969.

# ACKNOWLEDGMENT

The author wishes to thank his advisor, Professor Sylvian R. Ray, for his advice, guidance, and patience in the preparation of this thesis.

The author also wishes to thank Mrs. Mariam Coleman for typing the final draft of the thesis and Mr. Stanley Zundo for preparing the figures included in the thesis.

TABLE OF CONTENTS

# LIST OF FIGURES

## INTRODUCTION

Because of the numerous uses of ferrite materials in computer technology, especially in the coincident current memory area, much work has been done in an attempt to explain the observed behavior of the materials in terms of their physical properties. These attempts have taken the form of mathematical equations which predict what the voltage output waveform of a ferrite specimen will be under specified conditions of drive.

The problem here will be to produce the observed voltage output waveform of a ferrite core fully switched from an initially saturated condition by simulating the domain growth activity on a microscopic scale. It is hoped that this will provide some assistance in determining which of the models of the flux reversal process that have been proposed is more nearly correct.

# 1. PROPERTIES OF FERRITE MATERIALS

## 1.1 Polycrystalline Ferrites

Ferrites are ceramic ferromagnetic materials with the general chemical composition $YO \cdot FE_2O_3$ where Y is a divalent metal such as iron, manganese, magnesium, nickel, zinc, cadmium, cobalt, copper, aluminum, or a mixture of these. The ferrites crystalize into a cubic lattice structure which can be thought of as being made up of the closest possible packing of layers of oxygen ions with the metallic ions fit in the spaces left between the oxygen ions.

The metallic ions form bonds with the oxygen ions so that the otherwise free electrons of the metallic ions are not readily available for electrical conduction, thus eliminating the eddy current losses which are found in other magnetic materials. This is of significance here since, as a result of the high resistivity, the maximum rate of change of magnetization, which normally is limited by the eddy currents, can be large.

Polycrystalline samples of ferrites are prepared by a sintering process comprised basically of the following operations. The metal oxides and other compounds which are to form the ferrite are mixed and wet-milled, usually in a ball mill. The dried powder is prefired at a temperature of about 1000 $^{o}$C in order to produce the initial chemical reaction. The powder, after another milling and the addition of a binder, is pressed or extruded into the required shape. These products are then sintered at a temperature between 1200 and 1400 $^{o}$C, the exact temperature depending on the properties desired in the ferrites. In the sintering process the gas atmosphere in the furnace plays an important role, since it determines the degree of oxidation,

which has an important influence on the magnetic properties. It is in the sintering process that the crystal structure and its size and the porosity of the ferrite are determined. The longer the sintering, the larger the crystals and the more dense the ferrite. Typically, polycrystalline ferrites have a porosity of from 0.05 to 0.1. The voids existing in these ferrites have a large effect on the magnetic properties, since if the void is large enough, it can approximate a crystalline surface and thus be a source of the mobile domain walls which will be discussed later.

In a polycrystalline material, the directions of easy magnetization are not necessarily the same from grain to grain. However, since the ferrite materials in question have cubic structures, so that any given direction cannot be far from one of the three possible directions of easy magnetization, we can assume that the ferrites are essentially isotropic with regard to ease of magnetization. Later, when we consider the effects of magnetic fields on the ferrite materials, we will also assume that the sample is in the form of a toroid or a long rod parallel to the applied field.

## 1.2 Domains and Bloch Walls

Because of energy considerations, it is usually more advantageous for a ferromagnetic body, rather than to be uniformly magnetized, to divide itself into a number of regions of uniform magnetization, in which the magnetization vectors are parallel to a preferred direction, such that the demagnetizing fields, and thus the energy, are as small as possible. The resulting regions, or domains, of uniform magnetization are called "Weiss domains". These uniformly magnetized domains are separated by a thin layer in which the direction of the magnetization gradually changes from one direction to another. This transition boundary is known as a "Bloch wall".

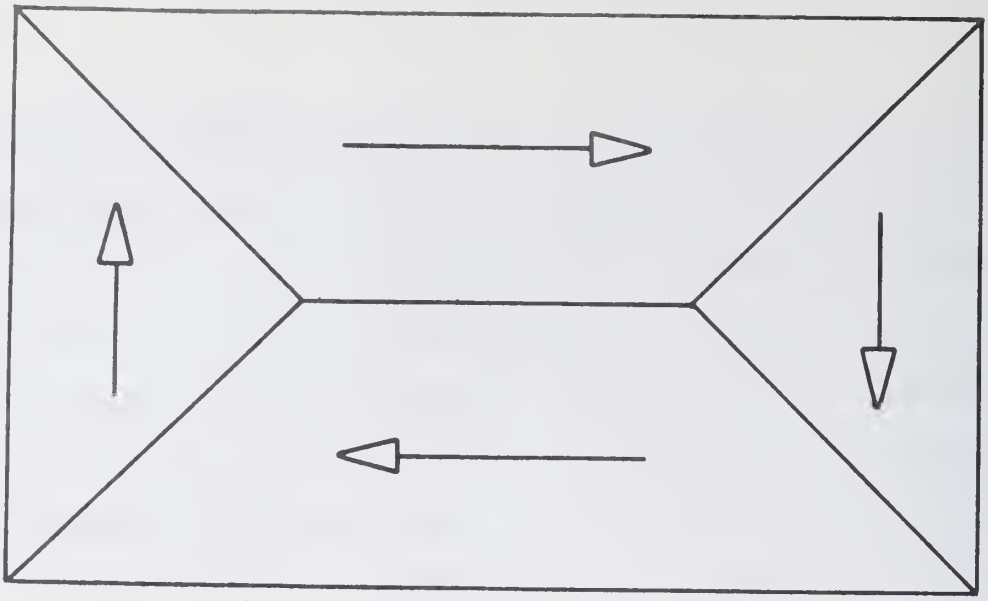

Figure 1.1 Example of Domain Walls

The change in angle of the magnetization vectors from one domain to another adjacent domain can be used to characterize the domain walls. In Figure 1.1, for example, there are four $90^{\circ}$ domain walls and one $180^{\circ}$ domain wall. Typically the walls have a small but non-negligible width (in the order of 100 $\mathring{A}$).

## 1.3 Domain Wall Motion

There are basically two ways the magnetization of a ferrite sample can be changed. The first is by the rotation of all the magnetization vectors simultaneously by the externally applied field. The second is by the motion of domain walls in the sample.

Flux changes due to rotation are the result of the torque caused by the magnetic field intensity, $\vec{H}$, acting on the magnetization, $\vec{M}$, according to the relation $\vec{T} = \vec{M} \times \vec{H}$. For a small field, only individual atomic spins are reversibly rotated. This is a small effect. To cause an irreversible rotation requires a much larger field. It has been estimated that the minimum field required is approximately four times the threshold field for materials such as

are considered here. However, the usual applications of these materials, such as in core memories, requires fields smaller than this. Thus we can assume the changes in magnetization are primarily caused by domain wall motion.

Goodenough (1954) also asserts that the principal cause of flux change may be assumed to be the motion of $180^{\circ}$ domain walls if the specimen does not have a special geometry or orientation of its axes of easy magnetization which would energetically favor the creation of many domains at right angles to the applied field.

Domains of reverse magnetization are formed at lattice imperfections. Among the imperfections which can serve as nucleating centers for new domains are granular inclusions, lammellar precipitates, grain boundaries, voids, and the crystalline surface. Goodenough (1954) has made a theoretical study of these imperfections and found that within the range of magnetic field strengths which are used in switch-core and coincident current memory applications, the grain boundaries are the primary source of mobile $180^{\circ}$ domain walls.

An externally applied magnetic field will try to alter the Weiss domain structure and, if it is strong enough, will cause the Weiss domains to vanish by eliminating the Bloch walls. This is accomplished by a movement of the Bloch wall. The magnetic field exerts a pressure on a Bloch wall which pushes the wall in such a direction that the domain with the magnetization in the same sense as the applied field becomes larger.

The wall will not be entirely free to move, however. With no externally applied field, a particular configuration of the Weiss domain structure will establish itself in a crystal. That configuration corresponds to a minimum of free energy. This means that the walls are bound with a certain stiffness

to their positions of equilibrium. This also means that when a Bloch wall is moving under the influence of a driving field and this driving field is removed, the wall will come to rest in such a way as to minimize the free energy.

Thus the change in magnetization of a sample of polycrystalline ferrite can be thought of as follows: starting with an initial configuration of Weiss domains, a magnetic field larger than the threshold field is applied causing the existing Bloch walls to move and new walls to be created in such a way as to increase the magnetization of the sample parallel to the applied field. A particular wall continues to move until either it meets another wall moving toward it, which annihilates both walls, or the driving field is removed and the walls come to rest in a new configuration.

## 2. MODELS OF DOMAIN WALL MOTION

### 2.1 Menyuk and Goodenough

Menyuk and Goodenough (1955) laid much of the ground work for the investigations that have followed of the flux switching processes in ferrites. They proposed that the magnetization reversal in polycrystalline ferrites is primarily due to the nucleation and growth of 180° Bloch walls. The walls took the form of ellipsoids with large eccentricities.

The first result they obtained was the equation of motion for the domain walls

$$\beta \frac{d\langle r\rangle}{dt} = 2I_S(H_m - H_o) \langle\cos\theta\rangle \ , \qquad (2.1)$$

where $\beta$ is the viscous-damping parameter for domain wall motion,

$r$ is the length of the domain semiminor axis,

$I_s$ is the spontaneous magnetization,

$H_m$ is the (constant) driving field,

$H_o$ is the threshold (maximum) field strength at which the wall velocity is zero, and

$\theta$ is the angle between the magnetization vector in the domain and the direction of the driving field $H_m$.

This relation assumes an ideally square input pulse and so is valid only for input pulses whose rise time is much less than the total switching time.

For the time rate of change of flux due to irreversible wall motion, Menyuk and Goodenough obtained the expression

$$\left(\frac{d\Phi}{dt}\right)_{irr} = \frac{16\pi I_s^2 \langle\cos\theta\rangle^3}{\beta} F(\langle r\rangle)(H_m - H_o) \qquad (2.2)$$

where $F(\langle r\rangle)$ is defined as $\partial A_c/\partial\langle r\rangle$, where $A_c$ is the cross-sectional area of the growing domains in the material with reversed magnetization.

Menyuk and Goodenough went on to explain that with a constant drive applied to the material, F(<r>) determines the shape of the flux switching curve. Since F(<r>) is a function of the wall positions, and the walls are assumed to accelerate to a constant average velocity in a time which is much smaller than the switching time, F(<r>) is a maximum when the area of the domain walls is a maximum. The wall surrounding a growing domain continues to move outward until it meets a similarly moving wall from another domain and is annihilated. Because of the random distribution of the growing domains throughout the material, F(<r>) decreases to zero with a Gaussian-like tail at larger values of r.

## 2.2 Haynes' Model

Haynes (1958) took the preceding work of Menyuk and Goodenough and extended the model using certain assumptions. Explicitly these assumptions were:

(1) Only irreversible wall motion will be treated,

(2) The nucleation field strength equals the threshold $H_o$,

(3) The number of nucleated domains is independent of $(H - H_o)$,

(4) The nucleation process and finite minimum size of a domain are neglected, and

(5) $\partial A_c/\partial \langle s \rangle$ is a function of domain wall position <s> and not of the velocity $d\langle s \rangle/dt$.

Further, Haynes assumed that the nucleating centers are distributed at random throughout the core volume, with an expectation of q nucleating centers per unit volume. This gives the Poisson distribution,

$$P(n,V) = \frac{(qV)^n}{n!} e^{-qV} \quad , \tag{2.3}$$

as the probability of occurrence of n nucleating centers in a volume V. Also, a constant k is defined, $k^3 \equiv 4\pi q/3\lambda$, so that $qV = k^3 s^3$, where $\lambda$ is the ratio of the semiminor to semimajor axes, and s is the length of the semiminor axis.

An expression is then derived for the rate of change of cross-sectional area as a function of s ($\partial A_c/\partial \langle s \rangle$). This expression is substituted into Equation 2.2 and integrated to obtain the result

$$\Phi = \langle \cos\theta \rangle \, \Phi_s \, (1 - 2e^{-qV}) \tag{2.4}$$

where $\Phi$ is the magnetic flux, and

$\Phi_s$ is the remanent value of the flux.

If the flux is normalized with respect to $\Phi_s \langle \cos\theta \rangle$ by defining

$$x = \frac{\Phi}{\Phi_s} \langle \cos\theta \rangle \quad , \tag{2.5}$$

we have

$$x = 1 - 2e^{-qV} = 1 - 2\exp[-k^3 \langle s \rangle^3] \tag{2.6}$$

Differentiating this expression and using Equations 2.1 and 2.2 the result is obtained

$$\frac{dx}{dt} = \frac{6kI_s}{\beta} \langle \cos\theta \rangle \, (H - H_o)(1 - x)\left(-\ln \frac{1 - x}{2}\right)^{2/3}. \tag{2.7}$$

Assuming a constant current excitation producing an applied field $H_m$, the output waveform exhibits the characteristic shape with a distinct peak value and peaking time. From Equation 2.7 it can be shown that a peak occurs at $x_p = 1 - 2e^{-2/3}$ or at $k\langle s \rangle_p = (2/3)^{1/3}$. Integrating Equation 2.1 eith $H = H_m$ and initial conditions $\langle s \rangle = 0$ at $t = 0$, gives

$$k\langle s \rangle = 2(I_s/\beta)k\langle \cos\theta \rangle (H_m - H_o)t \tag{2.8}$$

where the peaking time is

$$t_p = (2/3)^{1/3}\beta/2I_s k\langle\cos\theta\rangle(H_m - H_o). \tag{2.9}$$

Normalizing the time with respect to $t_p$, i.e., $t_1 = t/t_p$, and substituting into Equation 2.6 and differentiating we obtain

$$\frac{dx}{dt_1} = 4t_1^2 \exp[-(2/3)t_1^3] \tag{2.10}$$

which is a normalized response function representing all cases of constant current excitation. This equation will be used subsequently in comparing the various models.

## 2.3 Lindsey's Model

Lindsey (1959) also took the results of Menyuk and Goodenough and extended them. Instead of assuming the growing domains were elliptical with large eccentricity, Lindsey assumed the domains were expanding cylinders. The centers from which these domains started were scattered at random throughout the material. At time t = 0, all the domains were assumed to be of zero radius, at which time a field, $H_m$, was applied. The domains then expanded with radial velocity proportional to $(H_m - H_c)$, where $H_c$ is the coercive force.

Lindsey considered only a cross-section of the material perpendicular to the field, so that the domains became circles. He also assumed that the effect of not having the direction of easy magnetization parallel to the applied field was small and thus could be ignored. In his words:

> "...the only effect of having the direction of easy magnetization not parallel to the field would be to reduce the velocity of the Bloch walls, and this would not effect the shape of the output waveform basically."

With these assumptions, Lindsey proceeded to calculate the function F(r) in Equation 2.2. If r is the radius of a domain, v the velocity at which the walls move outward [proportional to $(H_m - H_c)$], and A is the area of the domain, then

$$\frac{dA}{dt} = \frac{d}{dt}(\pi r^2) = 2\pi r\frac{dr}{dt} = 2\pi rv \ . \qquad (2.11)$$

However, this does not take into account the possibility that part of the domain wall might have been annihilated through coalescence with other domains by the time the domain reaches a radius of r.

Consider an element of domain wall subtending an angle $d\theta$ at the center of the domain. If this element has not intersected a second domain by the time the radius of the domains is r, it implies that the center of a second domain cannot lie within a circle of radius r centered on the element $d\theta$. For, if the center of a second domain had been in this circle, the element $d\theta$ would not have gotten this far. Thus the probability that this element reaches a radius r is the probability of finding no other domain center within this circle of radius r. Since the centers are scattered at random, this is also the probability of finding a center in any circle of radius r. Let p be this probability. Then p also represents the proportion of such elements which reach a radius r. In this manner, then, Lindsey derived the following expression,

$$\frac{dA}{dt} = 2\pi rvp \ , \qquad (2.12)$$

which represents the rate of change of the area enclosed by the circles, divided by the number of circles.

The quantity p was then determined. If $\rho$ is the density of domain centers, then it can be shown that

$$p = \exp[-\pi r^2 \rho]. \tag{2.13}$$

Combining Equations 2.12 and 2.13 we have

$$\frac{dA}{dt} = 2\pi r v \exp[-\pi r^2 \rho] \tag{2.14}$$

But v is proportional to $(H_m - H_c)$, and the rate of change of the flux density is proportional to dA/dt, thus we have

$$\frac{dB}{dt} \propto (H_m - H_c) r \exp[-\pi r^2 \rho] \tag{2.15}$$

Comparing this equation with Equation 2.2, it can be seen that the required distribution function is given by

$$F(r) = Kr \exp[-\pi r^2 \rho] \tag{2.16}$$

where K is a constant.

If a constant applied field $H_m$ is assumed, so that v is constant, we have r = vt, and Equation 2.14 becomes

$$\frac{dA}{dt} = 2\pi v^2 t \exp[-\pi v^2 t^2 \rho] \tag{2.17}$$

and so

$$\frac{dB}{dt} = k_1 (H_m - H_c)^2 t \exp[-k_2 (H_m - H_c)^2 t^2] \tag{2.18}$$

$$= k_1 H^2 t \exp[-k_2 H^2 t^2] \tag{2.19}$$

where $k_1$ and $k_2$ are constants.

## 2.4 Comparison of the Models

We have seen that for constant current excitation Haynes obtained

$$\frac{dx}{dt_1} = 4t_1^2 \exp[-\tfrac{2}{3}t_1^3] \tag{2.20}$$

as the normalized response function. Rewriting this we have

$$\frac{d\Phi}{dt} = k_3 t^2 \exp[-k_4 t^3] \tag{2.21}$$

where $k_3$ and $k_4$ are constants. Thus the model using ellipsoids with large eccentricities as the shape of the growing domains of reverse magnetization results in a voltage output function of the form $t^2e^{-t^3}$.

Using circular domains in the flux switching process, Lindsey obtained the result

$$\frac{dB}{dt} = k_1H^2t \exp[-k_2H^2t^2] . \tag{2.22}$$

Combining the constants, we obtain

$$\frac{d\Phi}{dt} = k_1't \exp[-k_2't^2] . \tag{2.23}$$

Thus for Lindsey's model we have a voltage output function of the form $te^{-t^2}$.

Comparing Figure 2.1, which is an experimental voltage output waveform, with Figures 2.2 and 2.3, which are plots of $te^{-t^2}$ and $t^2e^{-t^3}$ respectively, it can be seen that Figure 2.2 corresponds more closely with the experimental waveform than does Figure 2.3. If the switching time, $t_s$, is defined as the time required for the output waveform to fall to 10% of its peak value, and the peaking time, $t_p$, has the obvious definition, then comparing the values of $t_s/t_p$ given on the respective Figures, it can be seen that Figures 2.1 and 2.2 agree more closely than Figures 2.1 and 2.3. Thus we see that there is some evidence of similarity between the results obtained from Lindsey's model and the results observed experimentally. On the experimental waveform, the region below 50ns no longer follows the predicted curve because of reversible effects not considered in this treatment.

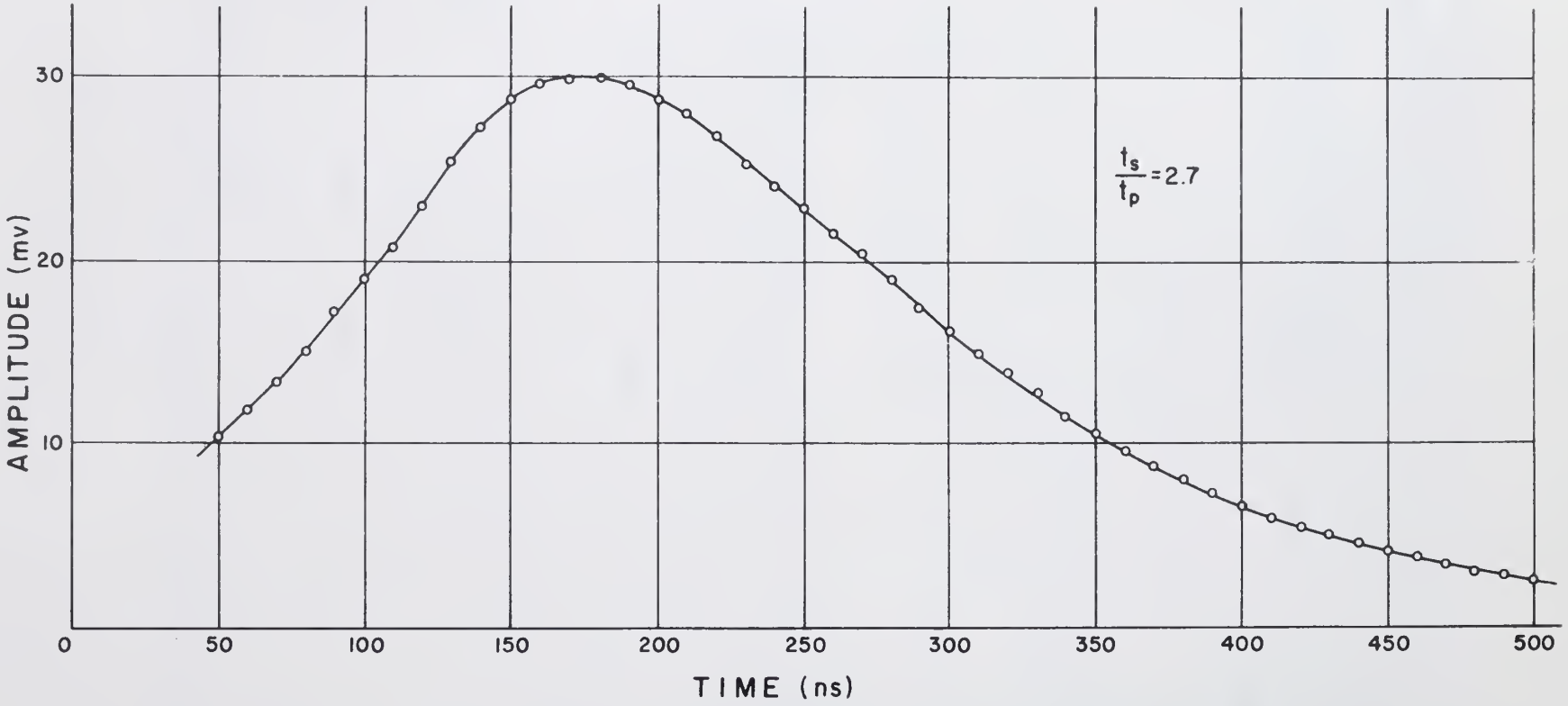


Figure 2.1 Experimental Full Switching Curve

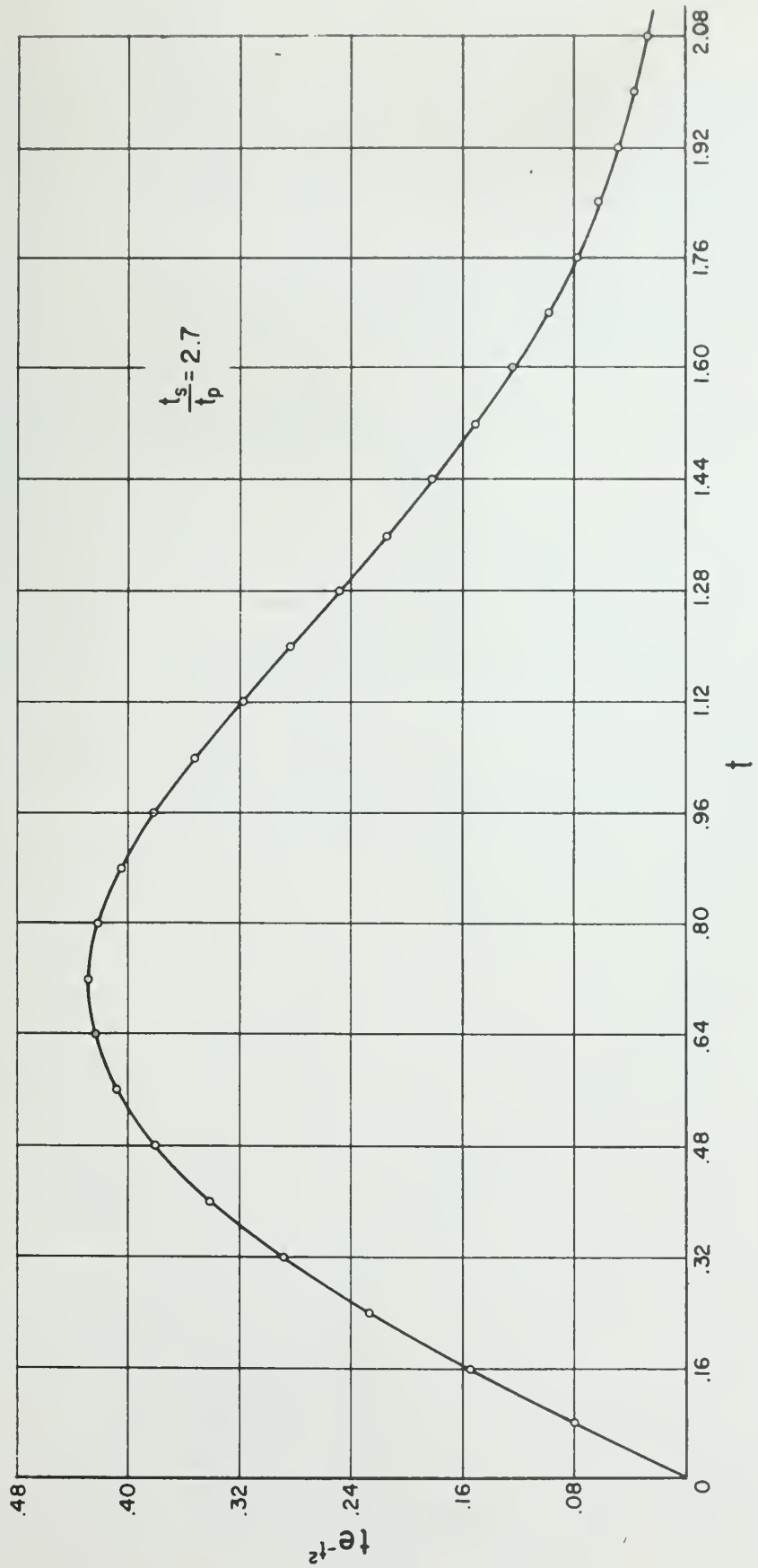


Figure 2.2 Plot of $te^{-t^2}$ vs. t

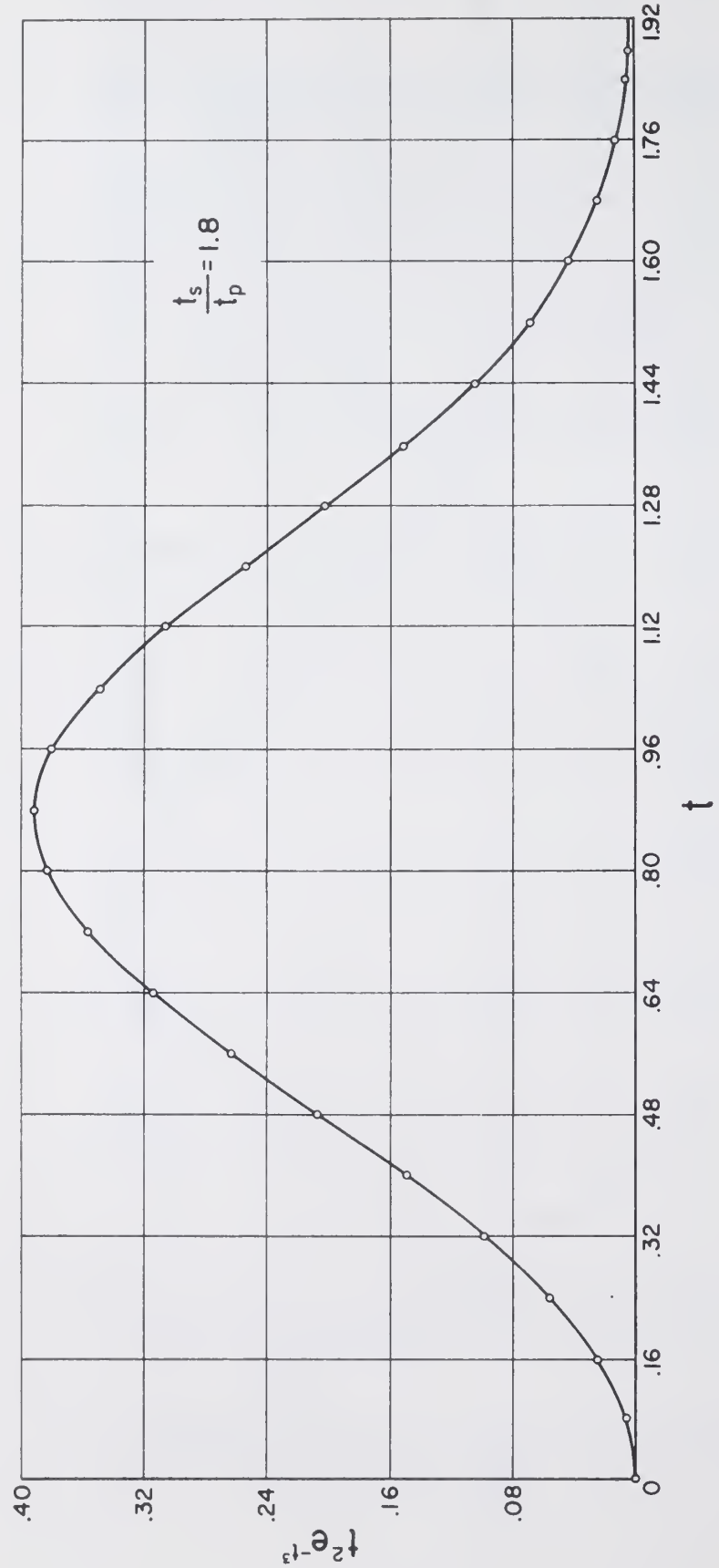


Figure 2.3 Plot of $t^2e^{-t^3}$ vs. t

Further corroboration comes from Ray (1961) who calculates a general flux switching equation for the case of constant current excitation. The equation is

$$\frac{dx}{dt} = 2nK^n t^{n-1} \exp[-(Kt)^n] , \qquad (2.24)$$

where K is a constant,

x is the normalized flux, and

$n > 1$.

Using experimental data, Ray calculates n to be from 1.8 to 2.2 for the range of drives normally used in memory applications, the range to which we have limited ourselves. This again would correspond to Lindsey's model.

Thus it would seem that the flux switching process can be modeled fairly closely using growing domains which are circular. An attempt then will be made to simulate the switching process using this model.

# 3. FLUX REVERSAL SIMULATION

## 3.1 Introduction

The following assumptions on the flux reversal process are basic to the simulation:

(1) The ferrite material is essentially isotropic with respect to the ease of magnetization.

(2) The changes in magnetization are primarily caused by the irreversible motion of $180^{\circ}$ Bloch walls.

(3) The material is in the form of a toroid or long rod parallel to the applied field.

(4) The applied field is a step function going from zero to some constant value at $t = 0$.

(5) The material is initially (i.e., at $t = 0$) magnetically saturated in a direction such as to diametrically oppose the field applied at $t = 0$.

(6) The nucleating centers are randomly scattered throughout the material.

(7) All domains are nucleated at $t = 0$ and have an initial radius of zero.

(8) The domain walls accelerate to a constant velocity in a negligible amount of time.

Using the model of cylindrical domains, and the assumptions given above, a program was written for the 360/75 in FORTRAN IV to simulate the flux switching process and output a rate of change of flux curve.

## 3.2 Simulation Details

In the simulation only a typical cross-section of ferrite material was considered. This was accomplished by performing the calculations on a 700 x 700 unit grid, considered to be perpendicular to the long axis of the domains, so that the problem was reduced to one of considering expanding circles.

The nucleating centers for the domains were scattered over the grid by using a random number generator with a uniform distribution for both coordinates of each point. The number of nucleating centers used was 88. This number was arrived at empirically as the approximate minimum number of centers needed to insure that the output waveform was fairly smooth.

The flux reversal process was limited to this grid without the need for considering edge effects by viewing the opposite edges of the square as coinciding. That is, any domain wall leaving the grid on the right, was introduced onto the grid on the left, and similarly for the top and bottom. For example, in Figure 3.1, the portion of the domain wall represented as the arc MN is considered, for calculating purposes, to exist at the left side of the grid as arc M'N' centered at A'. Similarly, for the domain centered at B, the arc PQ is considered to be at the lower right as arc P'Q' centered at B', the arc QR is considered to be at the lower left as arc Q'R' centered at B", and the arc RS is considered to be at the upper left as arc R'S' centered at B"', while the arc SP remains at the original location.

If A is the area and r the radius of one of the domains, then

$$\frac{dA}{dt} = \frac{d}{dt}(\pi r^2) = 2\pi r \frac{dr}{dt} = Cv \ , \qquad (3.1)$$

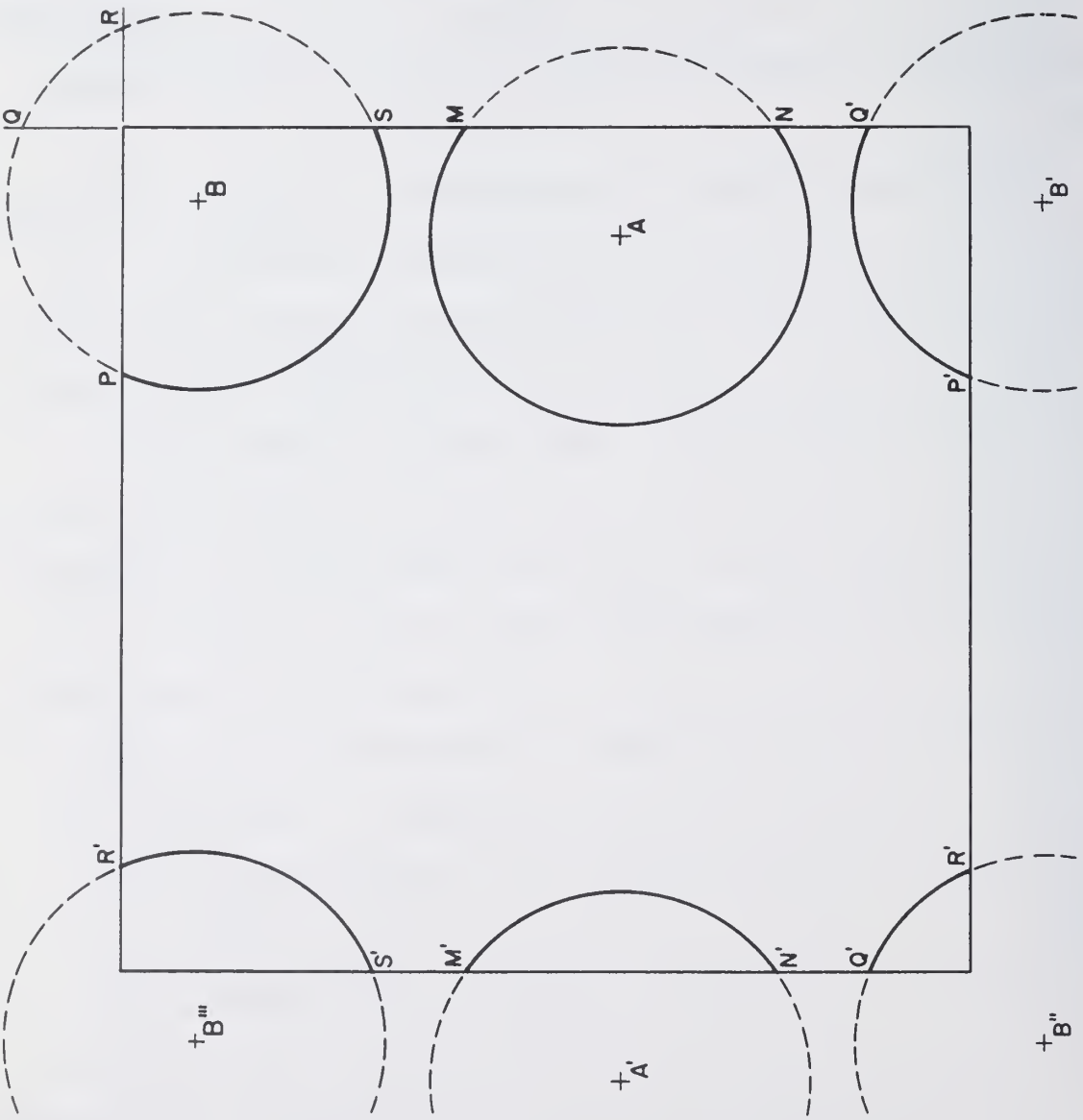


Figure 3.1 Simulation Grid Edge Effects

where C is the circumference and v is the wall velocity of the domain. As a domain grows, it will begin to coalesce with nearby similarly growing domains. Once this happens, it is no longer the complete circumference of the domain which is contributing to the change in area, dA/dt. The only contribution now comes from that portion of the circumference which has intersected no other domain. If we let C' be that portion of the circumference, we have

$$\frac{dA}{dt} = C'v \ . \tag{3.2}$$

This relation holds for all the domains on the grid.

If $\Phi$ is the total flux in the cross-section and $A_T$ the total area of all of the domains, then

$$\left.\frac{d\Phi}{dt}\right|_{t=t_1} \propto \left.\frac{dA_T}{dt}\right|_{t=t_1} , \tag{3.3}$$

or

$$\left.\frac{d\Phi}{dt}\right|_{t=t_1} = K \left.\frac{dA_T}{dt}\right|_{t=t_1} = KvC'_T\Big|_{t=t_1} \tag{3.4}$$

where K is a constant and $C'_T\Big|_{t=t_1}$ is the total length of all the domain circumferences which have not been intersected at $t = t_1$. Since v is also a constant over time and over all domains, we have

$$\left.\frac{d\Phi}{dt}\right|_{t=t_1} = K'C'_T\Big|_{t=t_1} \tag{3.5}$$

This gives us the rate of change of flux as a function of the total length of the domain walls which have not been intersected at a given time $t_1$.

For the simulation, the domain wall velocity was chosen to be one unit (on the 700 x 700 unit grid) per unit of time. This is a valid choice

since any other value of velocity would only change the output by a scale factor and would not affect the shape of the waveform. This means that the domain radius and the time always have the same numerical value, i.e., they both start at zero and are incremented by one for each successive step of the simulation.

The simulation proceeds, then, as follows. Starting at zero, the time and the domain radius take on successive integral values. At each value, the length of the circumference that had not yet been intersected is determined for each domain. These lengths are then totaled giving the value of $C'_T$ at that point in the flux reversal. Taking the constant K' to be unity, which again involves only a scale factor at the output, this value of $C'_T$ is output as the current value of $d\Phi/dt$. The time and the domain radius are then incremented, and the process is repeated. This continues until the calculated value of $d\Phi/dt$ falls below a predetermined level.

The results of the simulation are given in Table 3.1 and Figure 3.2. It can be seen that Figure 3.2 is the same shape as the experimental waveform of Figure 2.1. Here, again, the value of $t_s/t_p$ given in Figure 3.2 corresponds more closely to the values in Figures 2.1 and 2.2 than to the value in Figure 2.3.

An attempt was also made to simulate the partial switching process, that is, switching from an initially unsaturated state. This is accomplished by reversing the applied field at some point before the switching process is completed. This causes the existing domain wall segments to reverse their direction while new circular walls, growing outward, are created again at the nucleating centers. These two sets of walls move toward each other until they meet and all of the collapsing wall segments and an equal amount of the

| Time t | Rate of Change of Flux dΦ/dt | Time t | Rate of Change of Flux dΦ/dt | Time t | Rate of Change of Flux dΦ/dt |
|---|---|---|---|---|---|
| 0 | 0 | 34 | 9652 | 67 | 3198 |
| 1 | 552.9 | 35 | 9579 | 68 | 3007 |
| 2 | 1106 | 36 | 9468 | 69 | 2885 |
| 3 | 1659 | 37 | 9361 | 70 | 2786 |
| 4 | 2212 | 38 | 9184 | 71 | 2689 |
| 5 | 2759 | 39 | 8926 | 72 | 2571 |
| 6 | 3290 | 40 | 8684 | 73 | 2473 |
| 7 | 3828 | 41 | 8504 | 74 | 2314 |
| 8 | 4334 | 42 | 8319 | 75 | 2204 |
| 9 | 4811 | 43 | 8204 | 76 | 2067 |
| 10 | 5267 | 44 | 8033 | 77 | 1948 |
| 11 | 5715 | 45 | 7766 | 78 | 1822 |
| 12 | 6148 | 46 | 7635 | 79 | 1714 |
| 13 | 6541 | 47 | 7499 | 80 | 1618 |
| 14 | 6886 | 48 | 7196 | 81 | 1498 |
| 15 | 7224 | 49 | 6940 | 82 | 1346 |
| 16 | 7568 | 50 | 6712 | 83 | 1186 |
| 17 | 7871 | 51 | 6411 | 84 | 1014 |
| 18 | 8167 | 52 | 6109 | 85 | 896.3 |
| 19 | 8435 | 53 | 5835 | 86 | 768.5 |
| 20 | 8701 | 54 | 5595 | 87 | 626.6 |
| 21 | 8927 | 55 | 5363 | 88 | 540.1 |
| 22 | 9165 | 56 | 5189 | 89 | 453.8 |
| 23 | 9354 | 57 | 4974 | 90 | 395.8 |
| 24 | 9501 | 58 | 4767 | 91 | 371.9 |
| 25 | 9612 | 59 | 4566 | 92 | 348.5 |
| 26 | 9706 | 60 | 4420 | 93 | 324.8 |
| 27 | 9744 | 61 | 4288 | 94 | 302.2 |
| 28 | 9772 | 62 | 4092 | 95 | 280.5 |
| 29 | 9771 | 63 | 3922 | 96 | 244.5 |
| 30 | 9777 | 64 | 3705 | 97 | 179.1 |
| 31 | 9788 | 65 | 3524 | 98 | 131.0 |
| 32 | 9797 | 66 | 3362 | 99 | 97.29 |
| 33 | 9753 | | | | |

Table 3.1 Full Switching Results

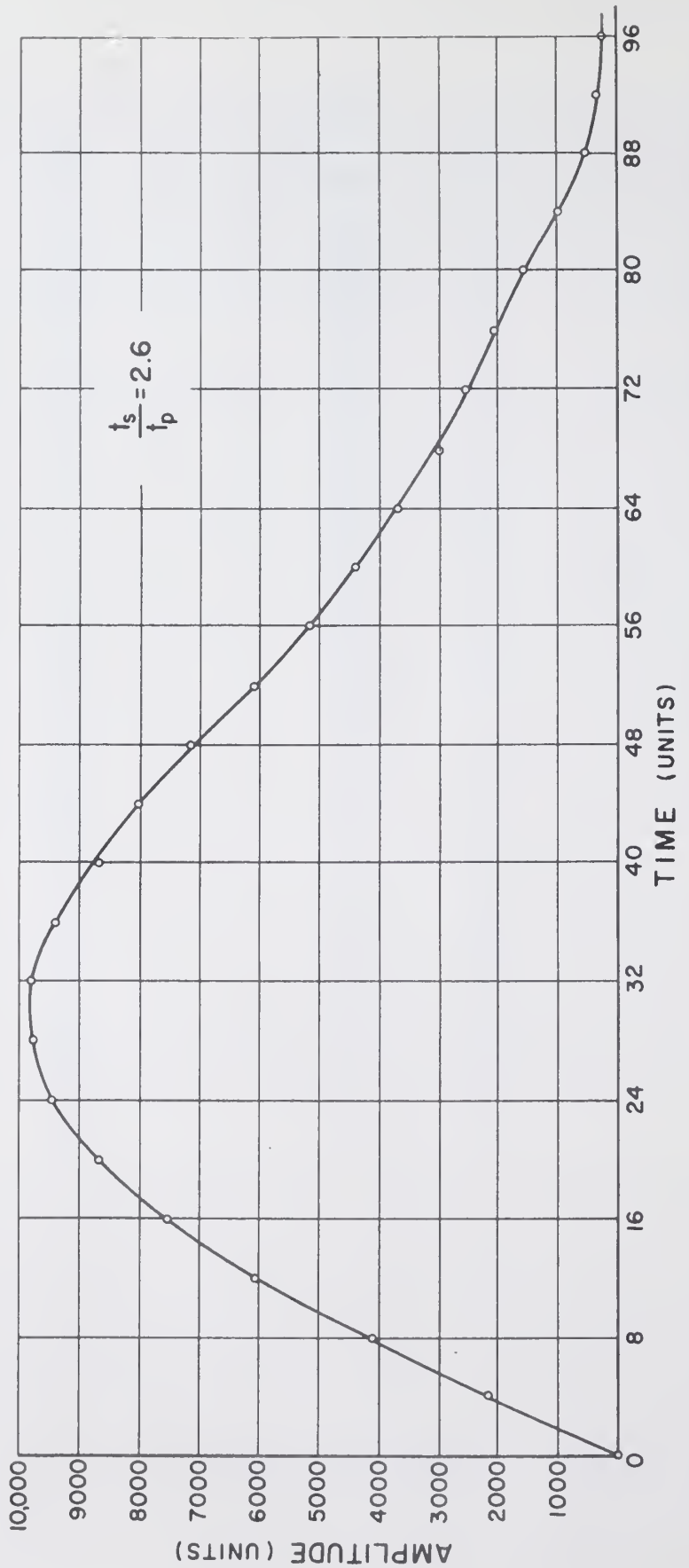


Figure 3.2 Simulated Full Switching Curve

growing walls are annihilated. The remaining wall segments complete their growth and eventual annihilation.

The results of this simulation, which utilized the same basic program as the full switching process, are given in Figure 3.3, along with an experimentally obtained curve in Figure 3.4. The results are unsatisfactory in that there is a discontinuity at t = 90 which does not appear on the experimental curve. This discontinuity results from all of the collapsing wall segments meeting the growing domains and being annihilated simultaneously. The two sets of walls meet simultaneously because all of the walls have the same velocity, and the collapsing wall segments retain their shape as arcs of the original domain walls.

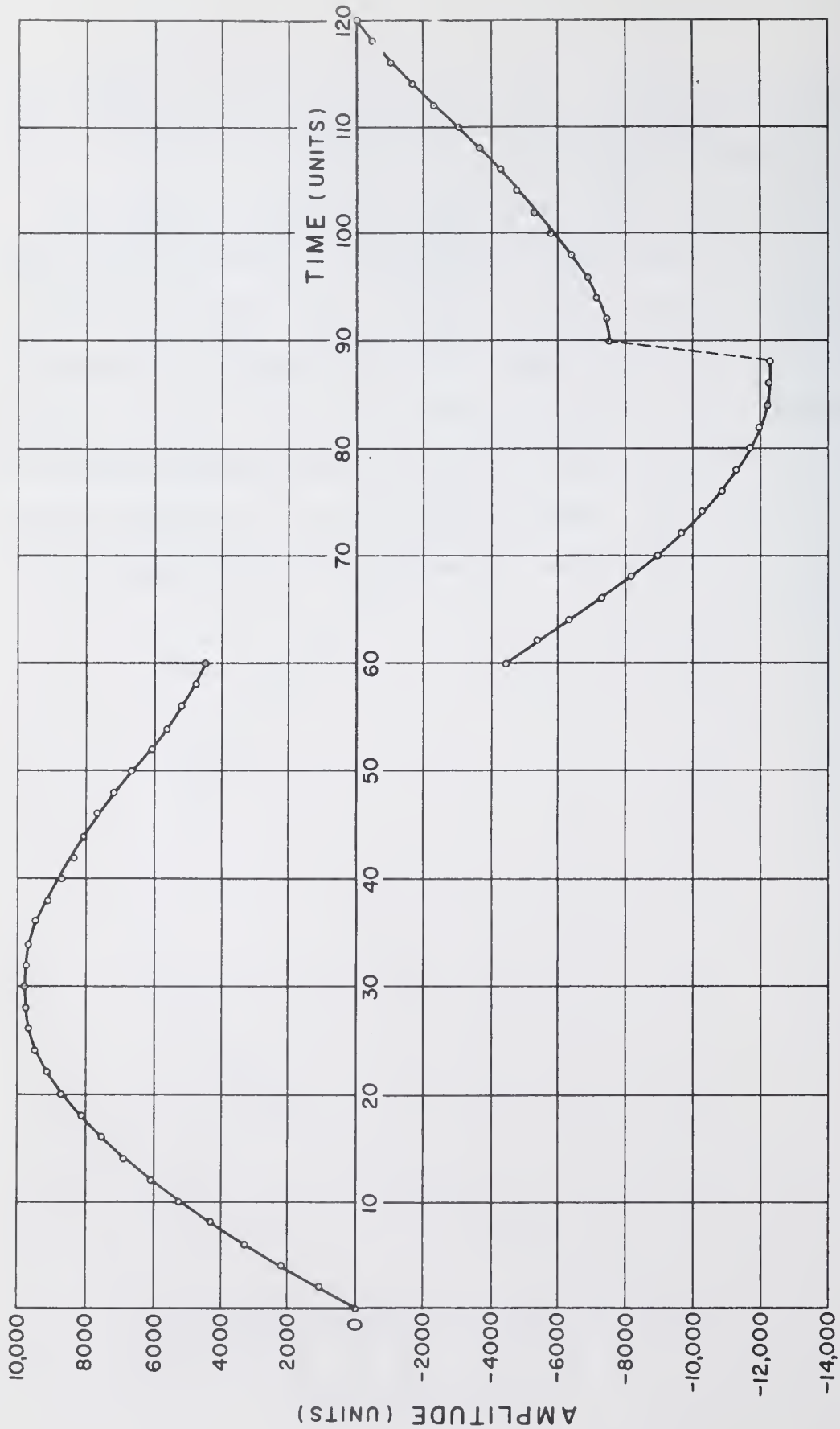


Figure 3.3 Simulated Partial Switching Curve

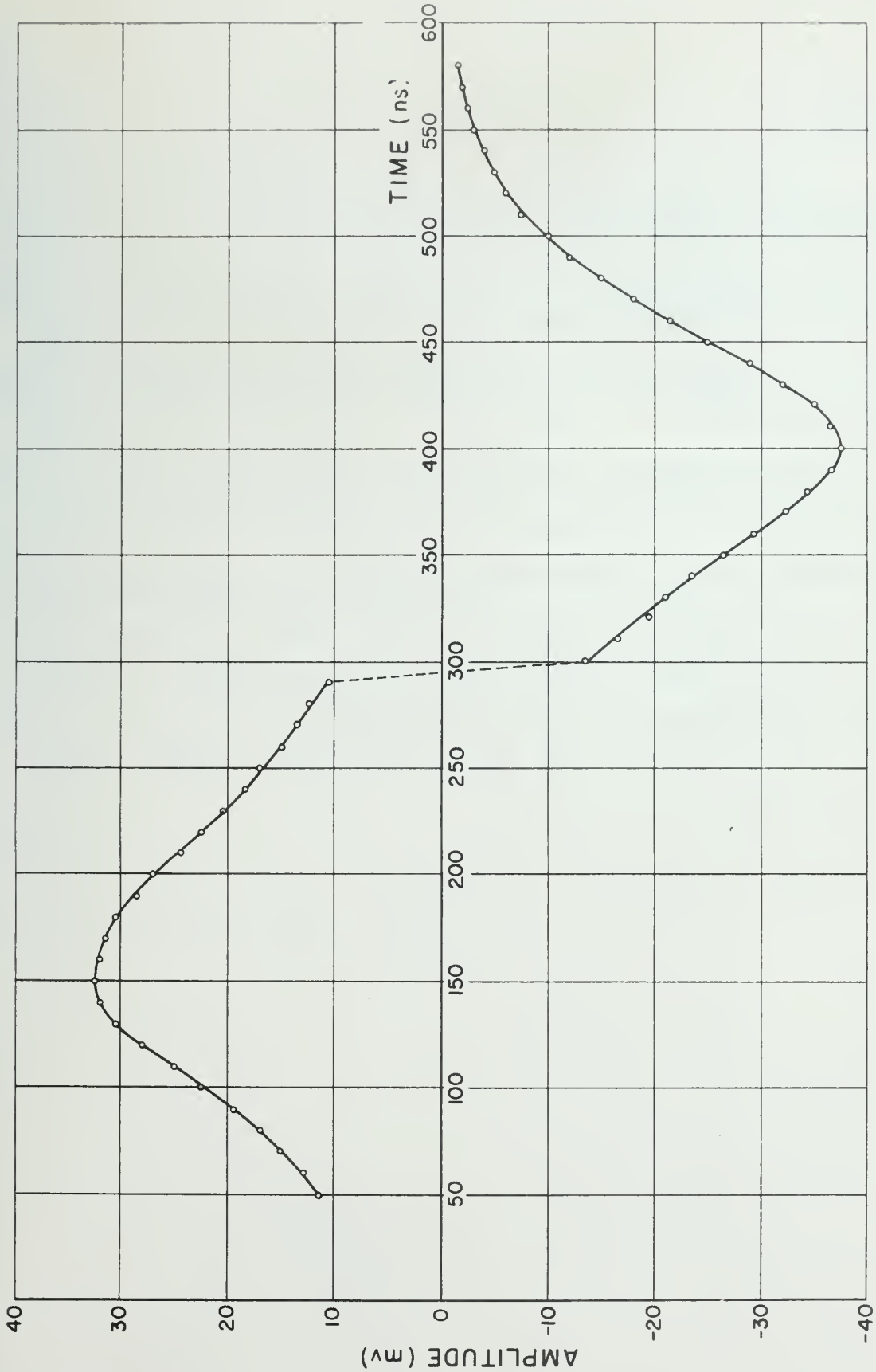


Figure 3.4 Experimental Partial Switching Curve

## CONCLUSION

For the case of a ferrite core fully switched from an initially saturated state, simulating the domain growth activity on a microscopic scale leads to results which coincide with the observed experimental results. These results also support Lindsey's contention that the flux switching process can be modeled using circular domains, rather than elliptical domains of large eccentricity.

The simulation of a ferrite core partially switched from an initially unsaturated state leads to a discontinuity in the output waveform which does not occur experimentally. To avoid this discontinuity, the simulation process would have had to allow the collapsing walls to change their shape continuously as they collapsed. This was beyond the model's capability since it handled the walls purely from the standpoint of their center and radius.

# LIST OF REFERENCES

Goodenough, J.B., (August 1954), "A Theory of Domain Creation and Coercive Force in Polycrystalline Ferromagnetics", Phys. Rev., Vol. 95, No. 4.

Haynes, M.K., (March 1958), "Model for Nonlinear Flux Reversals of Square-Loop Polycrystalline Magnetic Cores", Jour. of Appl. Phys., Vol. 29, No. 3.

Lindsey, C.H., (September 1959), "The Square-Loop Ferrite Core as a Circuit Element", Proc. of the Inst. of Elec. Engrs., Vol. 106, Part C, No. 10.

Menyuk, N. and Goodenough, J.B., (January 1955), "Magnetic Materials for Digital-Computer Components I. A Theory of Flux Reversal in Polycrystalline Ferromagnetics", Jour. of Appl Phys., Vol. 26, No. 1.

Nitzan, D., (September 1965), "Computation of Flux Switching in Magnetic Circuits", IEEE Transactions on Magnetics, Vol. MAG-1, No. 3.

Nitzan, D., (December 1966), "Models for Elastic and Inelastic Flux Switching", IEEE Transactions on Magnetics, Vol. MAG-2, No. 4.

Ray, S.R., (September 1961), "Engineering Model of a Partial Switching Effect in Ferrite Cores", PhD. Thesis, University of Illinois, Digital Computer Laboratory Report No. 111.

Smit, J. and Wijn, H.P.J., (1959), "Ferrites", John Wiley and Sons, New York.

Soohoo, R.F., (1960), "Theory and Application of Ferrites", Prentice-Hall, Inc., New Jersey.

# APPENDIX

The appendix contains the listing of the program used to simulate the full switching process.

```
C-----MAIN PROGRAM
      DIMENSION CTRLST(1ØØ,2)
      DIMENSION XCOORD(4Ø),YCOORD(4Ø),SDIST(4Ø),THETA(4Ø,2)
      DIMENSION BUFFP(1Ø)
      COMMON CTRLST, NUMCTR, XLIM, DENSE, M1, SDIST, XCOORD, I1, XC
      COMMON YC, RADIUS, THETA, NUMTH, TWOPI, TOTBDY, YCOORD, DIST
      COMMON LTIME
      COMMON IZ
      IB=1
      LTIME=Ø
      TOTBDY=Ø.
      XLIM=7ØØ.
      DENSE=1.8Ø41E-4
      TWOPI=6.2831853
      CALL CENTER
      DO 2 I=1,NUMCTR
      WRITE(6,9Ø)(CTRLST(I,J),J=1,2)
9Ø    FORMAT (1H ,2E11.4)
2     CONTINUE
      GO TO 15
5     TOTBDY=Ø.
      RADIUS=LTIME
27    IZ=1
29    DO 1Ø M1=1,NUMCTR
      CALL NEIGHB
      CALL CIRCI
      CALL SORT
      CALL BOUNDC
1Ø    CONTINUE
15    BUFFP(IB)=TOTBDY
      IF(IB-1Ø)35,2Ø,35
2Ø    WRITE(6,3Ø)LTIME,(BUFFP(I),I=1,IB)
3Ø    FORMAT (1HØ,I6, 1Ø(1X, E1Ø.4))
      IB=Ø
35    IB=IB+1
4Ø    IF(TOTBDY-1ØØ.)6Ø,6Ø,5Ø
5Ø    LTIME=LTIME+1
      GO TO 5
6Ø    IF(LTIME)7Ø,5Ø,7Ø
7Ø    IF(IB-1)2Ø,8Ø,2Ø
8Ø    CALL EXIT
      END
C-----CENTER GENERATOR SUBROUTINE
      SUBROUTINE CENTER
      DIMENSION CTRLST(1ØØ,2)
      DIMENSION XCOORD(4Ø),YCOORD(4Ø),SDIST(4Ø),THETA(4Ø,2)
      COMMON CTRLST, NUMCTR, XLIM, DENSE, M1, SDIST, XCOORD, I1, XC
      COMMON YC, RADIUS, THETA, NUMTH, TWOPI, TOTBDY, YCOORD, DIST
      COMMON LTIME
      NUMCTR=DENSE*XLIM**2
      DO 1Ø I1=1,NUMCTR
      CTRLST(I1,1)=XLIM*RAN3Z(Ø)
```

```
      CTRLST(I1,2)=XLIM*RAN3Z(Ø)
1Ø    CONTINUE
      RETURN
      END
C-----FIND NEAREST NEIGHBORS SUBROUTINE
      SUBROUTINE NEIGHB
      DIMENSION CTRLST(1ØØ,2)
      DIMENSION XCOORD(4Ø),YCOORD(4Ø),SDIST(4Ø),THETA(4Ø,2)
      DIMENSION ADJACE(1ØØ,18Ø)
      COMMON CTRLST, NUMCTR, XLIM, DENSE, M1, SDIST, XCOORD, I1, XC
      COMMON YC, RADIUS, THETA, NUMTH, TWOPI, TOTBDY, YCOORD, DIST
      COMMON LTIME
      IF(LTIME-1)13Ø,5,11Ø
5     DO 1Ø I1=1,4Ø
1Ø    SDIST(I1)=2.*XLIM
      DO 9Ø I1=1,NUMCTR
      IF(I1-M1)2Ø,9Ø,2Ø
2Ø    CALL PROXIM
      DO 45 I2=1,4Ø
      IF(DIST-SDIST(I2))45,4Ø,4Ø
4Ø    IF(I2-1)75,9Ø,75
45    CONTINUE
5Ø    I3=1
6Ø    IF(I3-I2)7Ø,8Ø,7Ø
7Ø    SDIST(I3)=SDIST(I3+1)
      XCOORD(I3)=XCOORD(I3+1)
      YCOORD(I3)=YCOORD(I3+1)
      I3=I3+1
      GO TO 6Ø
75    I2=I2-1
      GO TO 5Ø
8Ø    SDIST(I3)=DIST
      XCOORD(I3)=XC
      YCOORD(I3)=YC
9Ø    CONTINUE
      DO 1ØØ I3=1,4Ø
      I4=I3-1
      ADJACE(M1,3*I4+1)=XCOORD(I3)
      ADJACE(M1,3*I4+2)=YCOORD(I3)
1ØØ   ADJACE(M1,3*I4+3)=SDIST(I3)
      GO TO 13Ø
11Ø   DO 12Ø I3=1,4Ø
      I4=I3-1
      XCOORD(I3)=ADJACE(M1,3*I4+1)
      YCOORD(I3)=ADJACE(M1,3*I4+2)
12Ø   SDIST(I3)=ADJACE(M1,3*I4+3)
13Ø   RETURN
      END
C-----FIND THE CLOSEST IMAGE SUBROUTINE
      SUBROUTINE PROXIM
      DIMENSION CTRLST(1ØØ,2)
      DIMENSION XCOORD(4Ø),YCOORD(4Ø),SDIST(4Ø),THETA(4Ø,2)
```

```
      COMMON CTRLST, NUMCTR, XLIM, DENSE, M1, SDIST, XCOORD, I1, XC
      COMMON YC, RADIUS, THETA, NUMTH, TWOPI, TOTBDY, YCOORD, DIST
      COMMON LTIME
      CDIFF=CTRLST(I1,1)-CTRLST(M1,1)
      B=XLIM/2.
      IF(ABS(CDIFF)-B)1Ø,1Ø,2Ø
1Ø    XC=CTRLST(I1,1)
      GO TO 5Ø
2Ø    IF(ABS(CDIFF+XLIM)-B)3Ø,3Ø,4Ø
3Ø    XC=CTRLST(I1,1)+XLIM
      GO TO 5Ø
4Ø    XC=CTRLST(I1,1)-XLIM
5Ø    CDIFF=CTRLST(I1,2)-CTRLST(M1,2)
      IF(ABS(CDIFF)-B)6Ø,6Ø,7Ø
6Ø    YC=CTRLST(I1,2)
      GO TO 1ØØ
7Ø    IF(ABS(CDIFF+XLIM)-B)8Ø,8Ø,9Ø
8Ø    YC=CTRLST(I1,2)+XLIM
      GO TO 1ØØ
9Ø    YC=CTRLST(I1,2)-XLIM
1ØØ   DIST=SQRT((CTRLST(M1,1)-XC)**2+(CTRLST(M1,2)-YC)**2)
      RETURN
      END
C-----FIND CIRCLE INTERSECTION POINTS SUBROUTINE
      SUBROUTINE CIRCI
      DIMENSION CTRLST(1ØØ,2)
      DIMENSION XCOORD(4Ø),YCOORD(4Ø),SDIST(4Ø),THETA(4Ø,2)
      COMMON CTRLST, NUMCTR, XLIM, DENSE, M1, SDIST, XCOORD, I1, XC
      COMMON YC, RADIUS, THETA, NUMTH, TWOPI, TOTBDY, YCOORD, DIST
      COMMON LTIME
      COMMON IZ
      NUMTH=Ø
      DO 2Ø I1=1,4Ø
      IF(SDIST(I1)-2.*RADIUS)1Ø,2Ø,2Ø
1Ø    DX=XCOORD(I1)-CTRLST(M1,1)
      DY=YCOORD(I1)-CTRLST(M1,2)
      GAMMA=ATAN2(DY,DX)
      IF(GAMMA)11,12,12
11    GAMMA=GAMMA+TWOPI
12    PHI=ARCOS(SDIST(I1)/(2.*RADIUS))
      NUMTH=NUMTH+1
      THETA(NUMTH,1)=GAMMA-PHI
      THETA(NUMTH,2)=GAMMA+PHI
2Ø    CONTINUE
      GO TO (4Ø,3Ø),IZ
3Ø    WRITE(6,31)M1
31    FORMAT(1HØ,3HM1=,I3)
      DO 39 I=1,NUMTH
      WRITE(6,32)(THETA(I,N),N=1,2)
32    FORMAT(2E12.4)
39    CONTINUE
4Ø    RETURN
      END
```

```
C-----SORT THE INTERSECTION POINTS SUBROUTINE
      SUBROUTINE SORT
      DIMENSION CTRLST(1ØØ,2)
      DIMENSION XCOORD(4Ø),YCOORD(4Ø),SDIST(4Ø),THETA(4Ø,2)
      DIMENSION THETAL(12Ø),NWT(12Ø)
      COMMON CTRLST, NUMCTR, XLIM, DENSE, M1, SDIST, XCOORD, I1, XC
      COMMON YC, RADIUS, THETA, NUMTH, TWOPI, TOTBDY, YCOORD, DIST
      COMMON LTIME
      COMMON IZ
      DO 5Ø I1=1,NUMTH
      IF(THETA(I1,1))1Ø,4Ø,4Ø
1Ø    THETA(I1,1)=THETA(I1,1)+TWOPI
3Ø    THETA(I1,2)=THETA(I1,2)+TWOPI
4Ø    THETAL(2*I1-1)=THETA(I1,1)
      NWT(2*I1-1)=I1
      THETAL(2*I1)=THETA(I1,2)
      NWT(2*I1)=-I1
5Ø    CONTINUE
51    IF(NUMTH-1)11Ø,11Ø,52
52    LIM=2*NUMTH-1
55    INT=1
      DO 7Ø I1=1,LIM
      IF(THETAL(I1+1)-THETAL(I1))6Ø,7Ø,7Ø
6Ø    TEMP=THETAL(I1+1)
      THETAL(I1+1)=THETAL(I1)
      THETAL(I1)=TEMP
      NTEMP=NWT(I1+1)
      NWT(I1+1)=NWT(I1)
      NWT(I1)=NTEMP
      INT=I1
7Ø    CONTINUE
      IF(INT-1)8Ø,8Ø,75
75    LIM=INT-1
      GO TO 55
8Ø    GO TO (85,76),IZ
76    WRITE(6,77)
77    FORMAT(1HØ,12HSORTED TABLE)
      DO 79 I1=1,NUMTH
      I=NUMTH+I1
      WRITE(6,78)THETAL(I1),NWT(I1),THETAL(I),NWT(I)
78    FORMAT(2(E12.4,I1Ø,2ØX))
79    CONTINUE
85    LIM=2*NUMTH
      INT=1
      NUMTH=Ø
      NACC=Ø
      DO 1ØØ I1=1,LIM
      NACC=NACC+NWT(I1)
      IF(NACC)9Ø,9Ø,1ØØ
9Ø    NUMTH=NUMTH+1
      THETA(NUMTH,1)=THETAL(INT)
      THETA(NUMTH,2)=THETAL(I1)
```

```
      INT=I1+1
      NACC=Ø
      GO TO 1ØØ
1ØØ   CONTINUE
      GO TO (1Ø1,111),IZ
111   WRITE(6,112)
112   FORMAT(1HØ,15HEND THETA TABLE)
      DO 114 I1=1,NUMTH
      WRITE(6,113)(THETA(I1,I),I=1,2)
113   FORMAT(2E12.4)
114   CONTINUE
1Ø1   DO 13Ø I2=1,NUMTH
      DO 129 I3=1,2
      TEMP=THETA(I2,I3)+TWOPI
      IF(THETA(NUMTH,2)-TEMP)131,12Ø,12Ø
12Ø   THETA(I2,I3)=Ø.
129   CONTINUE
13Ø   CONTINUE
131   IF(I3-2)14Ø,132,132
132   THETA(NUMTH,2)=TWOPI
14Ø   IF(I2-1)11Ø,11Ø,141
141   I4=NUMTH-I2+1
      DO 142 I5=1,I4
      I6=I2+I5-1
      THETA(I5,1)=THETA(I6,1)
      THETA(I5,2)=THETA(I6,2)
142   CONTINUE
      NUMTH=I4
11Ø   RETURN
      END
C-----CALCULATE LENGTH OF BOUNDARY SUBROUTINE
      SUBROUTINE BOUNDC
      DIMENSION CTRLST(1ØØ,2)
      DIMENSION XCOORD(4Ø),YCOORD(4Ø),SDIST(4Ø),THETA(4Ø,2)
      COMMON CTRLST, NUMCTR, XLIM, DENSE, M1, SDIST, XCOORD, I1, XC
      COMMON YC, RADIUS, THETA, NUMTH, TWOPI, TOTBDY, YCOORD, DIST
      COMMON LTIME
      COMMON IZ
      ANGLE=Ø.
      IF(NUMTH)3Ø,21,1Ø
1Ø    DO 2Ø I1=1, NUMTH
2Ø    ANGLE=ANGLE+THETA(I1,2)-THETA(I1,1)
      BDY=RADIUS*(TWOPI-ANGLE)
      GO TO 23
21    BDY=RADIUS*TWOPI
23    GO TO (31,24),IZ
24    WRITE(6,25)M1,BDY
25    FORMAT(1HØ,3HM1=,I3,3X,4HBDY=,E12.5)
      WRITE(6,26)NUMTH
26    FORMAT(1HØ,6HNUMTH=,I3)
      IF(NUMTH)3Ø,31,27
27    DO 28 I1=1,NUMTH
```

```
28    WRITE(6,29)(THETA(I1,I),I=1,2)
29    FORMAT(2E12.4)
31    TOTBDY=TOTBDY+BDY
3Ø    RETURN
      END
```

Form AEC-427
(6/68)
AECM 3201

U. S. ATOMIC ENERGY COMMISSION

# UNIVERSITY-TYPE CONTRACTOR'S RECOMMENDATION FOR DISPOSITION OF SCIENTIFIC AND TECHNICAL DOCUMENT

*( See Instructions on Reverse Side )*

1. AEC REPORT NO.

COO-1018-1192-Report No. 358

2. TITLE

Modeling of Domain Growth Activity in Polycrystalline Ferrites

3. TYPE OF DOCUMENT (Check one):

- [x] a. Scientific and technical report
- [ ] b. Conference paper not to be published in a journal:
  - Title of conference _____
  - Date of conference _____
  - Exact location of conference _____
  - Sponsoring organization _____
- [ ] c. Other (Specify) _____

4. RECOMMENDED ANNOUNCEMENT AND DISTRIBUTION (Check one):

- [x] a. AEC's normal announcement and distribution procedures may be followed.
- [ ] b. Make available only within AEC and to AEC contractors and other U.S. Government agencies and their contractors.
- [ ] c. Make no announcement or distrubution.

5. REASON FOR RECOMMENDED RESTRICTIONS:

6. SUBMITTED BY: NAME AND POSITION (Please print or type)

Richard Paul Harms, Research Assistant

Organization

Department of Computer Science
University of Illinois
Urbana, Illinois 61820

Signature Richard P Harms

Date November 19, 1969

FOR AEC USE ONLY

7. AEC CONTRACT ADMINISTRATOR'S COMMENTS, IF ANY, ON ABOVE ANNOUNCEMENT AND DISTRIBUTION RECOMMENDATION:

8. PATENT CLEARANCE:

- [ ] a. AEC patent clearance has been granted by responsible AEC patent group.
- [ ] b. Report has been sent to responsible AEC patent group for clearance.
- [ ] c. Patent clearance not required.